

Reinforcing Effects of Natural Micro-Particles on the Dynamic Impact Behaviour of Hybrid Bio-Composites Made of Short Kevlar Fibers Reinforced Thermoplastic Composite Armor

Edison E. Haro, Akindele G. Odeshi, Jerzy A. Szpunar

Abstract—Hybrid bio-composites are developed for use in protective armor through positive hybridization offered by reinforcement of high-density polyethylene (HDPE) with Kevlar short fibers and palm wood micro-fillers. The manufacturing process involved a combination of extrusion and compression molding techniques. The mechanical behavior of Kevlar fiber reinforced HDPE with and without palm wood filler additions are compared. The effect of the weight fraction of the added palm wood micro-fillers is also determined. The Young modulus was found to increase as the weight fraction of organic micro-particles increased. However, the flexural strength decreased with increasing weight fraction of added micro-fillers. The interfacial interactions between the components were investigated using scanning electron microscopy. The influence of the size, random alignment and distribution of the natural micro-particles was evaluated. Ballistic impact and dynamic shock loading tests were performed to determine the optimum proportion of Kevlar short fibers and organic micro-fillers needed to improve impact strength of the HDPE. These results indicate a positive hybridization by deposition of organic micro-fillers on the surface of short Kevlar fibers used in reinforcing the thermoplastic matrix leading to enhancement of the mechanical strength and dynamic impact behavior of these materials. Therefore, these hybrid bio-composites can be promising materials for different applications against high velocity impacts.

Keywords—Hybrid bio-composites, organic nano-fillers, dynamic shocking loading, ballistic impacts, energy absorption.

I. INTRODUCTION

NATURAL fiber reinforced polymeric matrix composites are gaining considerable attention in the construction, military and automotive industries. These natural fiber composites are biodegradable and may contain organic fillers, which can further enhance their mechanical properties. Obtaining a strong interface between organic fillers and the polymer matrix has been a challenge that is being overcome with the addition of compatibilizers such as maleic anhydride. Earlier studies indicated that lack of good compatibility between natural fillers and polymer matrix adversely affect

mechanical properties such as impact and tensile strength of the organic filler reinforced plastic composites [1].

The hybridization of organic fiber reinforced composites by using inorganic fillers has also proved to be a promising method to enhance the interface between components and improve the mechanical strength and impact properties of polymer matrix composites [2], [3]. Hybrid composites containing more than two types of reinforcements (fibers and micro-fillers) have been developed and reported to exhibit improved performance [4]. These composites named hybrid bio-composites can be prepared using natural reinforcements (coir, bast, leaf, hardwood, cellulosic fillers) and synthetic fibres (glass, carbon, Kevlar, boron) incorporated in a polymer matrix [5], [6]. For example, Burgueno et al. [7] experimented with hybrid bio-composites made of green and raw hemp particles incorporated in a single polymer resin, and then impregnated the mixture into short jute fibers, glass strand mat and unidirectional carbon fibers. This resulted in composites with improved stiffness and strength.

In another study, the hybridization effects of short glass fibers and wood flour as reinforcements in thermoplastic matrix composites was evaluated by Valente et al. [1]. They reported improved flexural strength as a result of hybridization of glass fiber (20 wt. %) reinforced polymer LDPE (50 wt. %) with wood flour (30 wt. %). However, increasing the wood flour content above 30 wt. % led to a decrease in flexural strength. Hybridization of inorganic particles and short-fibers in a thermoplastic matrix is widely studied. For example, short-glass-fiber (SGF) reinforced polypropylene (PP) and short-carbon-fiber-reinforced polypropylene (PP) composites were investigated by Fu et al. [8]-[11]. The results of these studies confirm improvement of composites' strength, fracture resistance and impact capability in comparison to their polymer matrix. Fu and Lauke [8] investigated the effects of inorganic particles (calcite) and short glass fibers reinforced acrylonitrile-butadiene-styrene (ABS) terpolymer matrix, they concluded that toughness and strength of the composites can be enhanced by incorporation of glass short fibers and addition of calcite particles to ABS resin.

Yeung and Rao [12] investigated the mechanical behavior of Kevlar fibers reinforced thermoplastic composites using styrene acrylonitrile, acrylonitrile butadiene styrene and polyethylene resins as matrices and reported significant improvement in the tensile, compressive and flexural strength

E. E. Haro is with the Departamento de Ciencias de la Energía y Mecánica, Universidad de las Fuerzas Armadas ESPE, PO BOX 171-5-231B, Sangolquí, Ecuador (corresponding author, phone: 593-989055432; e-mail: eeharo@espe.edu.ec).

A. G. Odeshi and J. A. Szpunar are with the Department of Mechanical Engineering, University of Saskatchewan, 57 Campus Drive, Saskatoon, SK S7N 5A9 Canada (e-mail: ago145@mail.usask.ca, jerzy.szpunar@usask.ca).

of the thermoplastic as a result of reinforcement with Kevlar-49 [12]. Kevlar fibers have also been used to reinforce polypropylene (PP) to develop thermoplastic composites with improved ballistic resistance for use in protective armors [13]. The use of Kevlar pulp as reinforcement for thermoplastic polyimide composites was studied by Li [14], [15], and the results indicated improved tensile strength and wear resistance, which is optimum when the content of Kevlar pulp is 15 wt.%. The objective of this research project is to evaluate the effects of the addition of organic micro-particles (chonta palm wood) to Kevlar short fibers reinforced HDPE on the tensile properties, impact resistance, water absorption behavior, and crystallinity of the resulting hybrid composites.

II. MATERIAL AND EXPERIMENTAL PROCEDURE

A. Selection of Materials

High density polyethylene (SCLAIR 2909) used in this study as the polymer matrix was supplied by NOVA Chemicals. Its density is 0.962 g/cm^3 and it has a melt mass flow rate (MFR) of 1.3 g/min (D-1238-79 ASTM standard) at 190°C . HDPE has better energy absorption capacity and higher strength than low-density polyethylene (LDPE) and low-linear-density polyethylene (LLDPE) under dynamic compression load [16]. Kevlar short fibers (#544 Kevlar®) used as first reinforcement was supplied by Fibre Glast Developments Corporation. The fiber length ranged between 0.5 and 1 mm, and its density ranges between 0.048 and 0.16 g/cm^3 . Chonta palm wood (*Bactris gasipaes*) used as the natural micro-filler is one of the hardest woods in the Amazon region and its applications in various fields are discussed in previous publications [17], [18]. This natural fiber was provided by Indubalsa S.C. (Ecuador) in rectangular wood pieces, 150 mm long and 30 mm wide. The thickness ranged between 15 and 25 mm.

B. Sample Preparation

The as-received HDPE pellets were milled in a Retsch knife grinding machine using a 1 mm sieve under a continuous flow of carbon dioxide to avoid temperature rise during milling, which can alter the properties of the HDPE. This initial milling of HDPE was done to ensure homogeneous mixing of HDPE with Kevlar pulp and the micro-fillers. The moisture in the Kevlar® pulp was removed by heating at 105°C in an electric oven for 24 hours.

The as-received rectangular pieces of the chonta palm wood were cleaned and cut into small chips. The initial moisture content of the wood chips was measured using a Wagner moisture meter (MMC220, Oregon - US). This was determined to be 40 wt. % before drying and a significant reduction in moisture content was therefore necessary. The wood chips were heat-treated at 105°C for 24 h to reduce the moisture content. The dried chonta palm pieces were then milled using the Retsch knife grinding mill with a sieve size of 0.75 mm. The obtained chonta palm wood powder had particle sizes in the range between 500 and $750 \mu\text{m}$. These chonta palm powder was further dried in Supermatec (Hotpack) industrial electric

oven for 24 h at 105°C in order to reduce the moisture content of the wood microparticles to less than 1 wt.%. Moisture content was obtained by measuring the initial weight of wood chips (before milling) and the final weight of wood powder (after milling and drying process). A higher percentage of moisture will result in a porous composite.

The preliminary mixing of the components (micro-fillers/ Kevlar pulp/HDPE) before the extrusion process was done using a rotatory type mixer (National hardware, Dresden, ON) at a speed of 90 RPM for 15 minutes. After the preliminary mixing, the material was extruded in a parallel twin screw extruder (SHJ-35). The extrusion process has been frequently used to produce hybrid composites consisting of reinforcing fillers and thermoplastic matrix [8]-[11], [19]. The goal of the extrusion process is to produce a uniform distribution of the reinforcements (fillers/Kevlar pulp) within the polymer matrix. A screw rotating at 215 RPM drove the mixture through the barrel. The operating parameters such as motor current, melt pressure, motor speed, and feeder speed are 13.1 A, 0.5 MPa, 215 RPM and 50 RPM, respectively. The line temperature was varied in the following sequential order 140-150-155-160-170-175-180-185-220 $^\circ\text{C}$. The molten mixture was passed through a long needle-shaped die and hardened by a subsequent cooling by water immersion and air flow to form long noodles. These noodles were pelletized using a cooling strand LQ-60 pelletizer to obtain cylindrical pellets with a thickness ranging from 2 to 5 mm. The pellets were dried in an electric oven at 75°C for 48 hours, and then subsequently cured in a fluid bed dryer at 55°C for 30 minutes to eliminate any remaining moisture. The pellets were weighed before and after drying, and the moisture content of the pellets was estimated to be about 0.6 wt. %.

Finally, the pellets were subjected to compression molding to form 20 cm x 20 cm x 0.5 cm plates. During compression molding, 200 g of pellets were compressed at a constant pressure of 8.08 MPa at 160°C for 10 min. The resulting hybrid bio-composite plates were water-cooled for 30 min while the applied pressure was maintained to ensure good dimension stability. Similar manufacture procedures were followed in previous studies, when hybrid materials produced by addition of different types of micro- and nano-fillers to Kevlar pulp reinforced HDPE were developed for use in hybrid composite armors and tested under high velocity impacts [20].

C. Hybrid Bio-Composites Characterization

1. Mechanical Characterization

The tensile strength and the Young modulus of the specimens were determined using a 5500 R model Instron universal testing machine at room temperature according to ASTM D638 (type IV) standards [21]. The average dimensions of the rectangular specimens are 196 mm x 13.4 mm x 5 mm. Testing was carried out at a cross-head speed of 5 mm/min. A high resolution extensometer with a fixed gage length of 50 mm was attached to the test specimens to obtain reliable strain measurements for Young modulus determination.

2. Water Absorption

The water absorption test for the hybrid bio-composites was

performed according to ASTM D570 standard [22]. Rectangular specimens, 76.2 mm long by 25.4 mm wide and 5 mm thickness, were investigated by immersion in distilled water at 22 °C for two and twenty-four hours. The samples were weighed before and after immersion while the amount of water absorbed was determined as follows:

$$WA (\%) = \frac{W_1 - W_0}{W_1} \times 100\% \quad (1)$$

where WA is, the water absorbed (%), W0 and W1 represent the weights before and after water immersion (gm).

3. Dynamic Shock Loading Test

The dynamic impact test was conducted using an instrumented split Hopkinson pressure bar (SHPB). Rectangular specimens, 10 mm x 10 mm x 5 mm, were rapidly compressed between the incident and transmitter bars in this apparatus when a striker bar fired by a light gas gun struck the other end of the incident bar. Both the incident and transmitter bars (19 mm in diameter) were made of 7075-T651 aluminum alloy. In this study, the striker bar was fired at pressures of 50, 60, and 70 kPa, striking the incident bar at a momentum of 4.0, 6.8 and 8.7 kg.m/s, respectively. Five specimens were tested under each testing condition and the data reported in impact test results are averages of these five tests. The impact momentum generated average strain rates ranging between 900 and 2800 s⁻¹ in the specimens. The elastic waves produced by the impact travelled through the bars and were captured by strain gages mounted on them. These were amplified by the strain amplifier and recorded on a mixed signal digital oscilloscope connected to the strain conditioner/amplifier. More detailed description of this equipment is provided elsewhere [20], [23], [24]. Based on the strain pulses captured by the strain gages, the stress, strain and strain rates were calculated using the following equations [23]-[25]:

$$\sigma = \left(\frac{A_B}{A_S} \right) E_B \cdot \epsilon_T \quad (2)$$

$$\epsilon = -2 \left(\frac{C_B}{L_S} \right) \int_0^t \epsilon_R dt \quad (3)$$

$$\dot{\epsilon} = -2 \left(\frac{C_B}{L_S} \right) \epsilon_R \quad (4)$$

where A_B and A_S are the cross-sectional areas of the bars and specimen respectively. E_T and E_R are the transmitted and reflected strain pulses respectively, C_B is the velocity of elastic waves in the bars, E_B is the elastic modulus of the bar material. L_S and t represent the initial length of the specimen and deformation time, respectively.

4. Ballistic Impact Test

The ballistic impact resistance of the developed hybrid composite (target) was evaluated according to the NIJ-0101.06 standard [26]. The ballistic impact tests were conducted on square target plates (20 x 20 cm) with a thickness of 5 mm using a semi-automatic 9mm Beretta Cx4 Storm Rifle Luger, type FMJ ammunition with a mass of 124 g. The muzzle velocity and muzzle energy of this weapon are 381 m/s and 582 J, respectively [27], [28]. Six shots were fired at each target from a distance of 5 m. This distance is suitable to achieve stability and obtain reliable ballistic performance data [29]. The reported ballistic test data are averages of these six shots. The initial and residual velocities of the projectiles were respectively measured before and after bullet penetration to determine the energy absorbed by the targets. Ballistic precision chronographs (Caldwell) were used to measure the entry and residual velocities. A detail description of the ballistic impact test system is provided in earlier publications [20], [30], [31]. The initial impact energy, residual energy and absorbed energy were calculated based on the average initial velocity (V_i) of the projectile of mass m before impact and its residual or exit velocity (V_r) after perforating the target as follows [32], [33]:

$$\text{Initial (Impact) Energy (J)} = \frac{1}{2} m V_i^2 \quad (5)$$

$$\text{Residual energy of projectile after impact (J)} = \frac{1}{2} m V_r^2 \quad (6)$$

$$\text{Energy absorbed or dissipated (J)} = \frac{1}{2} m V_i^2 - \frac{1}{2} m V_r^2 \quad (7)$$

$$\% \text{ Energy dissipated} = \left(\frac{\text{Dissipated energy (J)}}{\text{Initial energy}} \right) \times 100 \quad (8)$$

III. RESULTS AND DISCUSSION

A. Microstructure and Physical Properties

Investigation of the microstructure of the obtained hybrid bio-composites was done using a Hitachi SU-6600 scanning electronic microscope (SEM) operating at an accelerated voltage of 15.0 kV. Specimens were gold coated using a Edwards S150B sputter coater. Typical microstructures of the obtain hybrid bio-composites are presented in Figs. 1 (a)-(d). K-1 specimens made of HDPE containing (10 wt. %) Kevlar pulp, show a uniform distribution of Kevlar short fibers and good bonding between HDPE and reinforcing components (Fig. 1 (a)).

In the hybrid bio-composite (Fig. 1 (b)-(d)), dispersed organic palm wood micro-particles of different sizes (0.5-0.75 mm) are observed clearly.

There is a random orientation of the micro-particles and short Kevlar fibers, it is possible to differentiate the increasing weight fraction of the added chonta palm micro-particles.

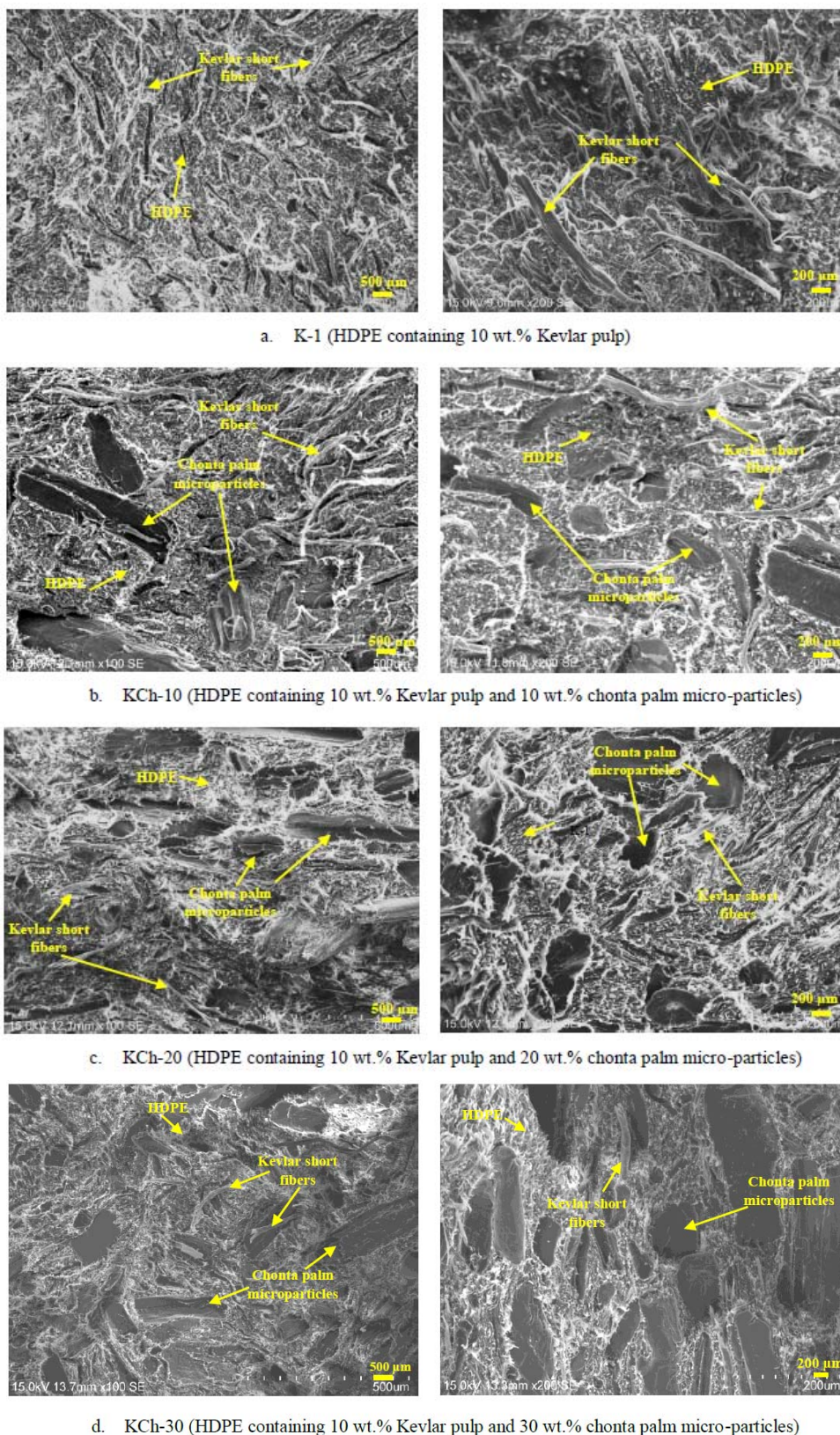


Fig. 1 SEM micrographs showing the transverse section of the hybrid bio-composites

The interphase region in the hybrid bio-composites developed is formed by the interaction between Kevlar short fiber/HDPE and wood palm micro-particles/HDPE. Similar characteristics were observed for all developed plates, i.e. they all exhibited a random orientation of both short Kevlar fibers and chonta palm wood micro-particles as well uniform distribution of the reinforcements. Since composite plates were maintained under pressure as the plates cooled from molding temperature to room temperature to ensure dimensional stability, uniform material properties at different locations in the plates is assumed. Moreover, test specimens were cut from the central regions while ballistic shots were also fired at central region to eliminate any possible effect of property variation at the edge of the plates.

TABLE I
EXPERIMENTAL DATA SHEET SHOWING COMPOSITION AND PHYSICAL PROPERTIES OF THE SYNTHESIZED HYBRID BIO-COMPOSITES

Targets configuration	K-1	KCh-10	KCh-20	KCh-30
Kevlar pulp (10%)	10%	10%	10%	10%
Chonta particles (wt.%)	-	10%	20%	30%
HDPE 2990 (wt.%)	90%	80%	70%	60%
Target weight average (g)	194±1.3	200±0.8	202±0.7	204±0.4
Target thickness ave. (mm)	5.5±0.1	5.1±0.1	4.8±0.2	4.7±0.2
Target areal density (g/cm ²)	0.49	0.50	0.51	0.51
Target density (g/cm ³)	0.88	0.99	1.05	1.09

K-1 = HDPE containing (10 wt.%) Kevlar pulp; KCh-10 = HDPE containing (10 wt.%) Kevlar pulp and (10 wt.%) Chonta palm micro-particles; KCh-20 = HDPE containing (10 wt.%) Kevlar pulp and (20 wt.%) Chonta palm micro-particle; KCh-30 = HDPE containing (10 wt.%) Kevlar pulp and (30 wt.%) Chonta palm micro-particles.

The physical properties of the hybrid composites developed in this study are presented in Table I. The density variations observed for the various category of hybrid bio-composites are mainly due to the difference in the densities of the organic micro-particles contained in the specimens. The results of water absorption test performed on the composites are summarized in Fig. 2. From these results, it is possible to observe that there exists a slight increase in water absorption with increase in the content of organic micro-fillers (wood palm flour). Water absorption was determined to be less than 0.06 % for all samples after soaking for 2 and 24 hours. This amount of water absorbed during this period is small and may not have significant effect on performance of the material. Samples K-1 and KCh-10 achieved the water absorption saturation of less than 0.03 wt. % after 2 hours of immersion and no further increase in weight due to absorbed water was observed after the 2-h exposure time. On the other hand, samples containing 20 and 30 wt. % chonta wood micro-particles (KCh-20 and KCh-30) absorbed more water in comparison to the other samples containing only Kevlar pulp (K-1) and those containing 10 wt. % wood particles (KCh-10). This can be attributed to exposure of higher content of the cellulosic particles which have greater tendency to absorb water. It has also been reported in previous investigations that the water resistance of HDPE composites are affected by the type, weight fraction and the size of natural fiber used as reinforcement [34], [35].

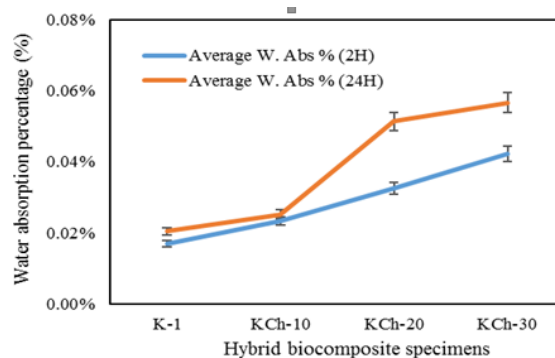


Fig. 2 Water absorption of hybrid bio-composite specimens

B. Mechanical Properties of Hybrid Bio-composites

The stress-strain curves of the hybrid bio-composites under quasi-static tensile loading are presented in Fig. 3, while tensile test results are summarized in Table II.

TABLE II
SUMMARY OF RESULTS OF THE TENSILE TEST CARRIED OUT ON THE HYBRID BIO-COMPOSITES

Hybrid composite specimens	Tensile strength σ (MPa)	Strain (ϵ) (%)	Young's Modulus (MPa)
K-1	22.2 ± 0.6	7.71 ± 1.0	616 ± 9.1
KCh-10	21.6 ± 0.9	6.49 ± 0.8	628 ± 16.2
KCh-20	17.4 ± 0.4	4.02 ± 0.2	678 ± 29.2
KCh-30	16.8 ± 1.3	2.99 ± 0.6	676 ± 12.9

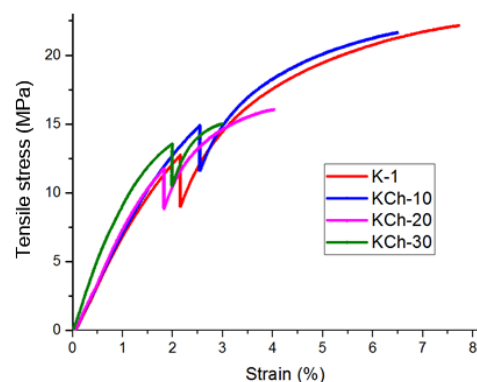


Fig. 3 Typical stress-strain curves of hybrid bio-composite specimens

Discontinuities can be observed in the stress-strain curves, which occurred when the tensile machine stopped at the end of elastic deformation and the extensometer used for precise strain measurement was removed. During the tensile testing, this extensometer was removed at the point of maximum elastic deformation, and subsequent elongation as the tensile load was further increased was based on the crosshead movement of the machine. The use of this extensometer enables accurate determination of the yield point and Young modulus of hybrid bio-composites.

The highest tensile strength value was recorded for K-1 specimens (HDPE composites containing only Kevlar short

fibers), which also exhibited the least tendency of fracture under tensile loading. This suggests a more efficient interaction and load transfer across the short Kevlar fiber/matrix interface. On the other hand, when a second filler (palm wood micro-particles) was added to the short Kevlar fibres reinforced HDPE composites, a reduction in tensile strength was observed. This result was observed to be the case with 10 % wood micro-particle addition (KCh-10) and for composites containing higher wood particle content (KCh-20 and KCh-30). This suggests that the presence of the wood particles affects the stress transfer between reinforcing Kevlar fibers and the continuous HDPE matrix. Other researchers [36], [37] have also reported that excessive reinforcements (fibers or particles) in composite materials can lead to saturation in the matrix. This saturation is produced when the reinforcements become located very close to each other, leading to agglomeration and a weak interface between matrix and the agglomerates, thereby causing tensile strength reduction due to hindered stress transfer between matrix and the reinforcement.

With respect to material stiffness, a marginal improvement in the Young modulus (2.0 – 10.1 %) was achieved by wood particle addition to the short Kevlar fiber reinforced HDPE. The highest stiffness was observed for KCh-20 specimens. This was slightly reduced as the wood particle content was raised from 20 to 30 % in the KCh-30 specimens. This suggests the optimum content of wood particle addition for enhanced stiffness is 20 %. It is evident from these findings that a positive hybridization effect can be achieved with respect to stiffness by the use of palm wood microparticle and short Kevlar fibers as reinforcements in a thermoplastic HDPE matrix.

C. Dynamic Mechanical Behavior of Hybrid Bio-composites under Impact Loading

The results of the dynamic impact test on the specimens developed are provided in Table III. The strain rates of the test specimens varied between 900 and 2700 s^{-1} depending on the impact momentum, which is determined by the firing pressure of the striker bar. The maximum flow stress is observed to be higher for the hybrid bio-composites compared with the control samples containing no wood particles.

The stress-strain curves of the hybrid bio-composites for various impact momentums of the projectile are presented in Fig. 4. The stress-strain curves indicate yield points that are, in most cases less than 100 MPa, depending on the impact momentum. Beyond the elastic limit, the stress-strain curves become non-linear.

Scanning electron microscopic micrographs of some of the damaged specimens after the impact test are presented in the Fig. 5. As the impact momentum increased, the intensity of damage in the specimens increased and finally specimen rupture occurred. The failure progression involved a(n extensive plastic deformation, crack initiation, and crack propagation until fracture. A significant increase in the areal dimensions and a considerable reduction in thickness of the impacted specimens were observed. This is attributed to the

extensive plastic deformation typical of the thermoplastic matrix under mechanical load [38].

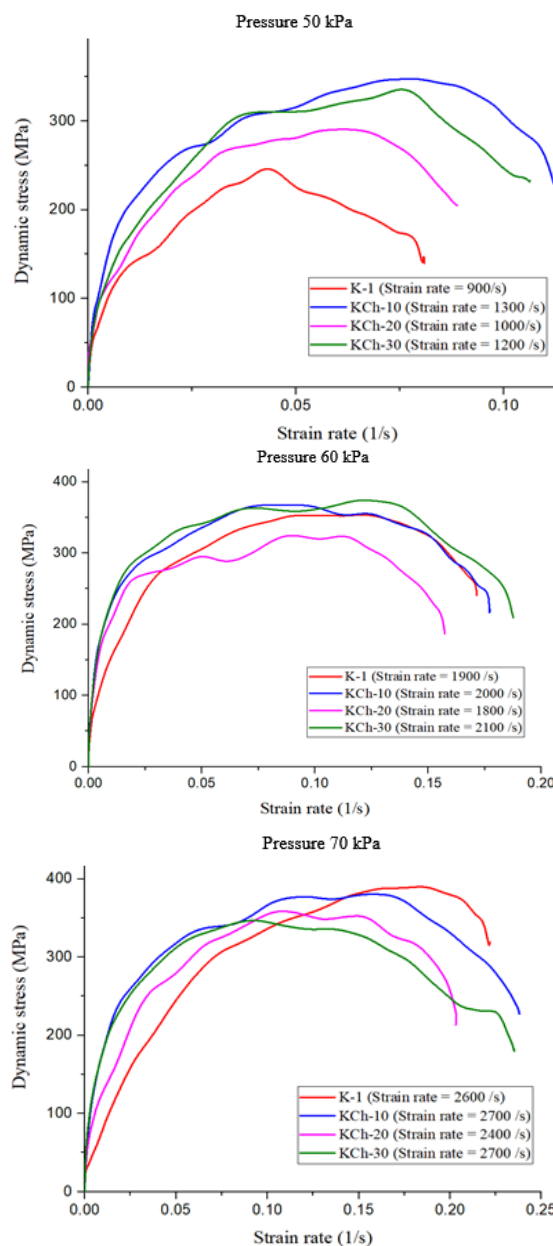


Fig. 4 Dynamic stress-strain curves of hybrid bio-composites under dynamic impact loading

All the hybrid bio-composites experienced an extensive plastic deformation without rupture when impacted at the lowest momentum of 4.0 kg.m/s (pressure 50 kPa.). This again can be traced to the plasticity of the thermoplastic matrix. As the impact momentum was raised to 6.8 kg.m/s (pressure 60 kPa.), small cracks were observed in the specimens. Crack initiations were observed to occur where there is micro-particle agglomeration. These cracks propagated along the direction of alignment of the particle-agglomerates. This suggests that

excessive accumulation of Kevlar short fibers or organic micro-fillers within specific areas of the HDPE matrix, can affect bonding with the HDPE matrix resulting in weak interface that can promote cracking and fracture under dynamic impact loading. When the impact momentum was increased further to 8.7 kg.m/s (pressure 70 kPa.), the K-1, KCh-20, and KCh-30 specimens ruptured completely under the impact load, but specimens containing chonta palm 10 wt. % (KCh-10) kept their structural integrity. This observation aligns well with the impact stress-strain data provided in Table III. Also, the SEM micrographs of the impacted specimens indicate Kevlar fibers breakage and matrix fracture in addition to debonding between matrix and reinforcements. Fiber bridging and fiber pull-out can be observed along the crack propagation paths.

TABLE III
MAXIMUM COMPRESSIVE STRESS AND STRAIN RATE OF HYBRID BIO-COMPOSITES UNDER DYNAMIC IMPACT LOADING

Pressure	Specimens	Max Strain rate (s ⁻¹)	Max Stress (MPa)
50 kPa 4.0 kg.m/s	K-1	900	247± 9.1
	KCh-10	1300	348± 5.8
	KCh-20	1000	291± 22.3
	KCh-30	1200	336± 16.6
60 kPa 6.8 kg.m/s	K-1	1900	354± 12.4
	KCh-10	2000	368± 9.5
	KCh-20	1800	325± 18.4
	KCh-30	2100	374± 24.2
70 kPa 8.7 kg.m/s	K-1	2600	390± 8.6
	KCh-10	2700	380± 11.9
	KCh-20	2400	359± 25.2
	KCh-30	2700	347± 18.1

Specimens after dynamic shock loading
(Impact momentum = 8.7 kg.m/s)

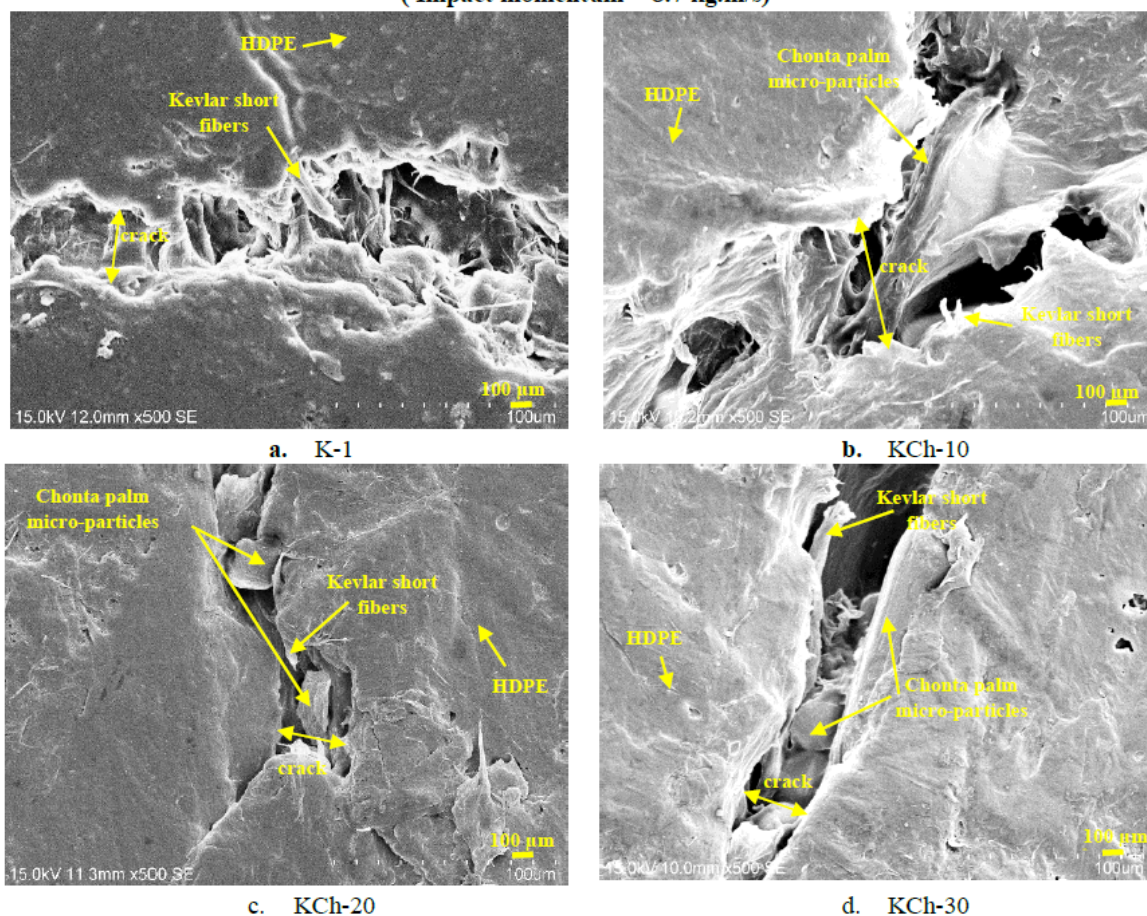


Fig. 5 Deformed and fractured of samples after dynamic shock loading

D. Energy Absorbed at Hybrid Bio-composite Targets under Ballistic Impact Tests

The results of the ballistic impact test indicating the initial and exit velocities of the projectile after penetration of the bio-composite targets developed in this study are provided in

Table IV. The average initial velocity of the projectile was determined to be 385 m/s, which is an average of six shots with a standard deviation of 6.2 m/s. The initial velocity is comparable to the muzzle velocity of 381 m/s for the same ammunition as provided in NATO specifications. In addition,

the initial average energy of the six shots was estimated to be 593 J, with a standard deviation of 19 J, which is also consistent with the original muzzle energy value of 582 J for that ammunition in the NATO specifications. Moreover, all the samples were tested using the similar conditions of distance, temperature, and firing. Here, the absorbed energy from the target represents the loss in kinetic energy as the projectile perforates the target, while the residual kinetic energy is the projectile energy that remains after the target is perforated by the projectile [39].

TABLE IV
BALLISTIC IMPACT DATA SHEET FOR THE VARIOUS HYBRID BIO-COMPOSITE TARGETS PRODUCED

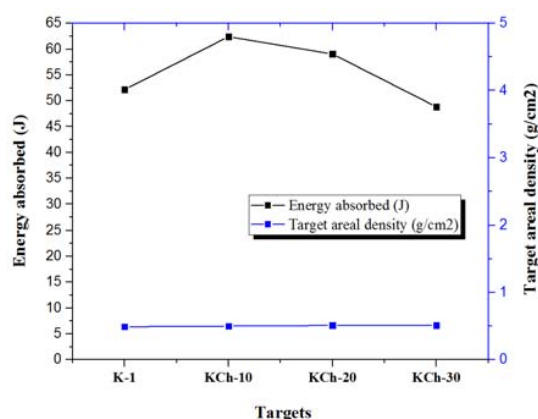
Targets	Initial Energy average (J)	Velocity measured after impacts average (m/s)	Energy absorbed at targets average (J)	Energy absorbed above that K-1 control samples
K-1	593 ± 19	367.9 ± 5.6	52.2 ± 16.3	0%
KCh-10	593 ± 19	364.5 ± 3.1	62.4 ± 9.0	20%
KCh-20	593 ± 19	365.6 ± 3.1	59.1 ± 9.0	13%
KCh-30	593 ± 19	369.1 ± 2.2	48.8 ± 6.5	-6%

Note: Initial velocity measured before impacts average was of 385 ± 6.2 (m/s)

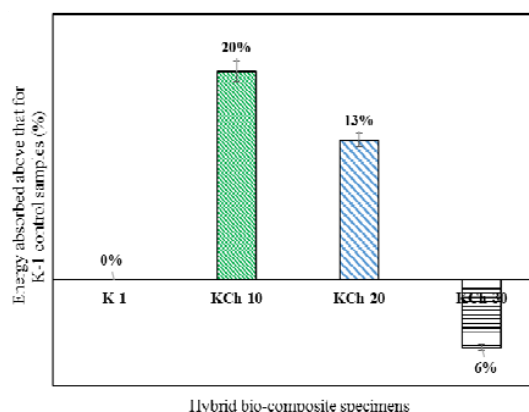
Fig. 6 (a) shows the energy absorbed by the various targets having similar target areal density. The plot of percentage increase in energy absorbed against the weight fraction of added wood particle is presented in Fig. 6 (b). The energy absorbed by the control specimens, Kevlar pulp reinforced HDPE (K-1), is estimated to be 52.2 J. A significant ballistic resistance enhancement was achieved in the hybrid bio-composite plates containing 10 wt. % of chonta palm micro-particles (KCh-10), which exhibit the highest energy absorption of 62.4 J. This is equivalent to 20 % improvement over control specimens K-1 with similar thickness and density. The KCh-20 specimens containing 20 wt. % chonta palm micro-particles exhibited a 13 % increase in the energy

absorption (59.1 J) over K-1 samples. These results can also be related to the improvements achieved in material stiffness. On the other hand, hybrid bio-composites containing 30 wt. % chonta palm micro-particles (KCh-30) absorbed only 48.8 J of impact energy which is 6 % lower than the energy absorbed by composites containing no wood particle addition. Therefore, 10 % chonta wood particles addition to Kevlar pulp/HDPE composite is considered the optimum wood particle content for best resistance to ballistic penetration. Higher amounts of the second reinforcement (milled wood fibers) can lead to an excessive accumulation of fibers or filler micro-particles in any region within the matrix. This will have detrimental effects on the impact resistance of the hybrid bio-composites. The saturation of wood particles is produced when the reinforcements become located very close to each other, leading to agglomeration, poor bonding, and a weak interface between agglomerated particles and the matrix. This accounts for the reduction energy absorbed observed for composite containing 20 and 30 wt. % wood particles.

The results of the SEM investigations of the transverse section of the perforations in the targets after the ballistic impact testing are presented in Fig. 7. These micrographs provide information on the deformation, penetration and the sequence of damage in the targets during ballistic impact. The deformation and penetration of the targets are influenced by the projectile shape (round nose), impact velocity as well as physical and mechanical properties of the targets. The damage sequence starts with an indentation on the frontal face of the target, which is produced by a localized stress at the point of impact. The pressure exerted by the projectile creates a small puncture. A ductile crater enlargement can be observed at the bullet entry orifice. Horizontal striations were observed on target perforation surface (Fig. 7 bullet entry orifice), which occurred by lands and grooves that come from the rifling process of the ogive.



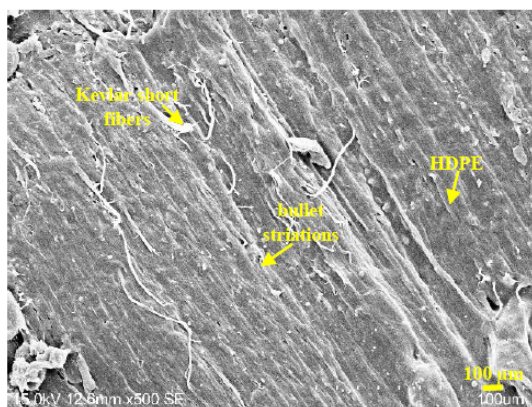
a) Energy absorbed by targets during ballistic testing of composites with similar density



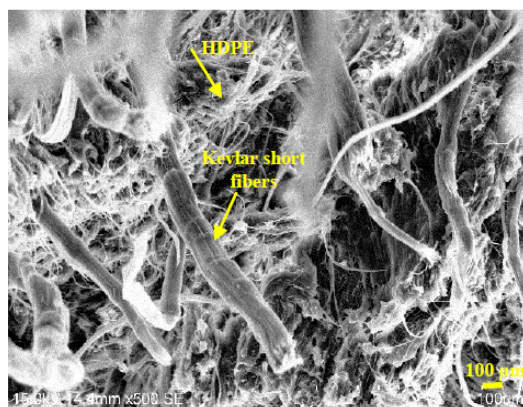
b) Improvements of the energy absorption compared to K-1 control sample (% increase)

Fig. 6 Energy absorbed by hybrid bio-composites containing chonta palm microparticles

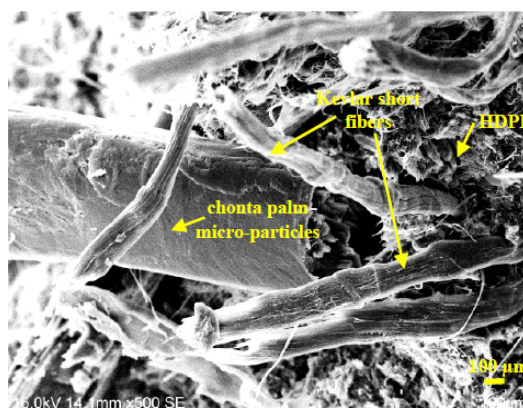
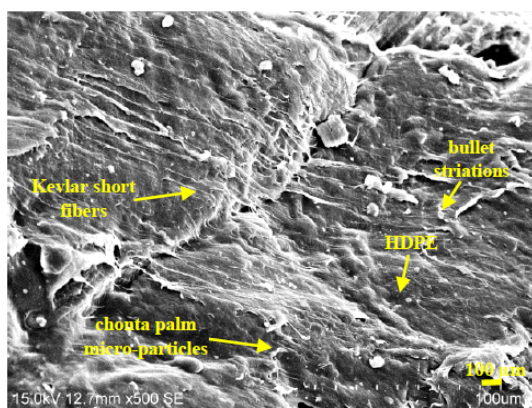
Bullet entry orifice



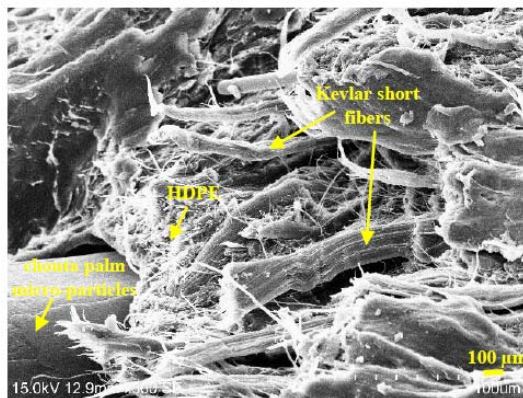
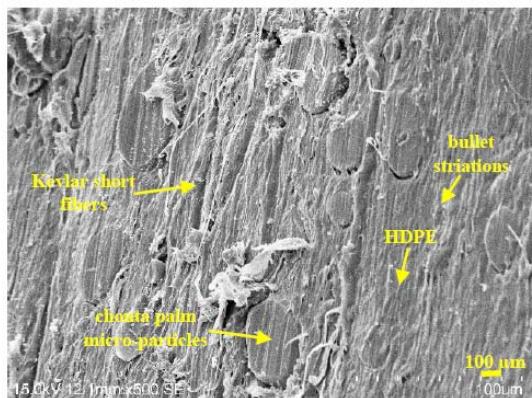
Bullet exit orifice



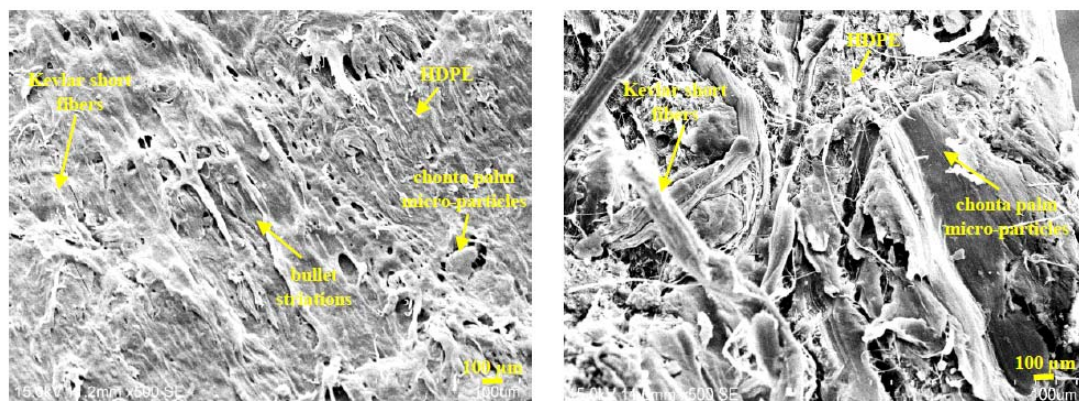
a. K-1



b. KCh-10



c. KCh-20



d. KCh-30

Fig. 7 Energy absorbed by hybrid bio-composites containing chonta palm microparticles

The impression marks are characteristics of bullet as it travels through the target. Fig. 7 also shows the bullet exit orifice, exhibiting a large material detachment indicated by short Kevlar fibers and chonta palm microparticles exposure. This fracture is associated with the projectile exit after the total penetration. Difference in behavior in terms of material detachment was observed in the targets, as a result of their different energy absorption capability and resistance against ballistic impacts. For example, the amount of fiber-pull out and material detachment in the KCh-10 and KCh-20 targets, was observed to be lower than for other specimens. This material behavior is in agreement with the energy absorption results presented in Table IV. The improved resistance to material detachment during perforation can be considered to be responsible for the greater energy absorption and better resistance to projectile penetration in these specimens.

IV. CONCLUSIONS

Hybrid bio-composites were prepared by incorporating organic micro-fillers into short Kevlar fibers reinforced HDPE matrix composite. The organic fillers used as second reinforcement are organic chonta palm wood micro-particles in different proportion (10, 20, and 30 wt. %). The effects of this second filler addition on the quasi-static tensile strength, crystallinity, dynamic compressive strength and ballistic impact resistance of the hybrid bio-composites were investigated. Material characterization showed that the addition of the micro-fillers reduces the tensile strength of the Kevlar short fiber reinforced HDPE. However, such addition improved the material stiffness. XRD analysis revealed that the crystalline structure of Kevlar fiber reinforced HDPE remained unchanged with the addition of the organic wood particles. However, the intensity of the crystalline peaks decreased with increasing content of the organic micro-fillers. Microstructural analysis indicated that the size of the organic micro-particles, their alignment and distribution could affect the bonding with Kevlar short fibers within HDPE matrix. The dynamic shock loading test revealed optimum impact resistance by hybrid composites containing 10 wt. % chonta

wood particles in addition to the short Kevlar fibers. An excessive accumulation of fibers or filler micro-particles in any region within the matrix will have detrimental effects on the impact resistance of the hybrid bio-composites, due to a formation of weak interface between agglomerated fibers or particles with the polymer matrix. Similarly, the results of the ballistic impact test revealed that the composites containing 10 wt. % of organic wood particles exhibited the highest capacity for energy absorption during ballistic impact. Reinforcing HDPE with Kevlar pulp and organic micro-fillers (not more than 10 wt. %) result in hybrid bio-composites with an enhanced performance under dynamic mechanical loading.

ACKNOWLEDGMENT

The authors wish to acknowledge the financial support of the Natural Sciences and Engineering Research Council (NSERC) of Canada and that of the National Secretary of Science and Technology of the Ecuador (SENESCYT) and Ecuadorian Army.

REFERENCES

- [1] M. Valente, F. Sarasini, F. Marra, J. Tirillò, and G. Pulci, "Hybrid recycled glass. fiber/wood flour thermoplastic composites: Manufacturing and mechanical characterization," *Composites Part A Applied Science Manuf.*, vol. 42, no. 6, pp. 649–657, 2011.
- [2] G. Cantero, A. Valea, I. Mondragon, A. Arbelaz, and B. Ferna, "Mechanical properties of flax fibre / polypropylene composites. Influence of fibre / matrix modification and glass fibre hybridization," vol. 36, pp. 1637–1644, 2005.
- [3] S. Mishra, A. K. Mohanty, L. T. Drzal, M. Misra, and S. Parija, "Studies on mechanical performance of biofiber / glass reinforced polyester hybrid composites," vol. 63, pp. 1377–1385, 2003.
- [4] T. P. Sathishkumar, J. Naveen, and S. Satheshkumar, "Hybrid fiber reinforced polymer composites – a review," *Journal of Reinforced Plastics and Composites*, vol. 33, no. 5, pp. 454–471, 2014.
- [5] M. Rivai, a. Gupta, M. R. Islam, and M. D. H. Beg, "Characterization of oil palm empty fruit bunch and glass fibre reinforced recycled polypropylene hybrid composites," *Fibers Polym.*, vol. 15, no. 7, pp. 1523–1530, 2014.
- [6] B. K. Deka and T. K. Maji, "Effect of Silica Nanopowder on the Properties of Wood Flour / Polymer Composite," *Polymer Engineering and Science*, vol. 52, no. 7, pp. 1516–1523, 2012.
- [7] R. Burgueno, M. J. Quagliata, A. K. Mohanty, G. Mehta, L. T. Drzal, and M. Misra, "Hybrid biofiber-based composites for structural cellular plates," *Compos. Part A Appl. Sci. Manuf.*, vol. 36, pp. 581–593, 2005.

- [8] S. Y. Fu and B. Lauke, "Characterization of tensile behaviour of hybrid short glass fibre calcite particle ABS composites," *Compos. Part A Appl. Sci. Manuf.*, vol. 29, no. 5–6, pp. 575–583, 1998.
- [9] S. Y. Fu, G. Xu, and Y. Mai, "On the elastic modulus of hybrid particle/short fiber/polymer composites," *Composites Part B: Engineering*, vol. 33, pp. 291–299, 2002.
- [10] S. Y. Fu, B. Lauke, E. Mader, C. Y. Yue, and X. Hu, "Tensile properties of short-glass-fiber- and short-carbon-fiber-reinforced polypropylene composites," *Compos. Part A Appl. Sci. Manuf.*, vol. 31, no. 10, pp. 1117–1125, 2000.
- [11] S. Y. Fu, B. Lauke, E. Mader, X. Hu, and C. Y. Yue, "Fracture resistance of short-glass-fiber-reinforced and short-carbon-fiber-reinforced polypropylene under Charpy impact load and its dependence on processing," *J. Mater. Process. Technol.*, vol. 89–90, pp. 501–507, 1999.
- [12] K. K. H. Yeung and K. P. Rao, "Mechanical properties of Kevlar-49 fibre reinforced thermoplastic composites," *Polym. Polym. Compos.*, vol. 20, no. 5, pp. 411–424, 2012.
- [13] A. Kumar, V. V. Chavan, S. Ahmad, and R. Alagirusamy, "International Journal of Impact Engineering Ballistic impact response of Kevlar ® reinforced thermoplastic composite armors," *Int. J. Impact Eng.*, vol. 89, pp. 1–13, 2016.
- [14] J. Li, "The Effect of Kevlar Pulp Content on Mechanical and Tribological Properties of Thermoplastic Polyimide Composites," *J. Reinf. Plast. Compos.*, vol. 29, no. 11, pp. 1601–1608, 2010.
- [15] J. Li, "The Effect of Carbon Fiber Content on the Mechanical and Tribological Properties of Carbon Fiber-Reinforced PTFE Composites," *Polym. Plast. Technol. Eng.*, vol. 49, no. 4, pp. 332–336, 2010.
- [16] M. F. Omar, H. M. Akil, and Z. A. Ahmad, "Effect of molecular structures on dynamic compression properties of polyethylene," *Mater. Sci. Eng. A*, vol. 538, pp. 125–134, 2012.
- [17] S. Graefe, D. Dufour, M. van Zonneveld, F. Rodriguez, and A. Gonzalez, "Peach palm (*Bactris gasipaes*) in tropical Latin America: Implications for biodiversity conservation, natural resource management and human nutrition," *Biodivers. Conserv.*, vol. 22, no. 2, pp. 269–300, 2013.
- [18] W. L. E. Magalhães, S. A. Pianaro, C. J. F. Granado, and K. G. Satyanarayana, "Preparation and characterization of polypropylene/heart-of-peach palm sheath composite," *J. Appl. Polym. Sci.*, vol. 127, no. 2, pp. 1285–1294, 2013.
- [19] M. S. Salit, "Tropical natural fibre composites: properties, manufacture and applications," *Engineering Materials*, Singapore: Springer, 2014.
- [20] E. E. Haro, A. G. Odeshi, and J. A. Szpunar, "The Effects of Micro- and Nano-Fillers' Additions on the Dynamic Impact Response of Hybrid Composite Armors Made of HDPE Reinforced with Kevlar Short Fibers," *Polym. Plast. Technol. Eng.*, vol. 0, no. 0, pp. 1–16, 2017.
- [21] ASTM, "ASTM: D638, Standard test method for tensile properties of plastics," *ASTM Stand.*, pp. 1–16, 2013.
- [22] D570, "Water Absorption of Plastics 1," *ASTM Stand.*, vol. 98, no. Reapproved 2010, pp. 25–28, 2014.
- [23] C. Weinong and S. BO, "Split Hopkinson (Kolsky) Bar: Design, Testing and Applications", *Mechanical Engineering Series*, Springer, vol. 1, 2013.
- [24] M. F. Omar, H. Md Akil, Z. A. Ahmad, A. A. M. Mazuki, and T. Yokoyama, "Dynamic properties of pultruded natural fibre reinforced composites using Split Hopkinson Pressure Bar technique," *Mater. Des.*, vol. 31, no. 9, pp. 4209–4218, 2010.
- [25] A. A. Tiarniyu, R. Basu, A. G. Odeshi, and J. A. Szpunar, "Plastic deformation in relation to microstructure and texture evolution in AA 2017-T451 and AA 2624-T351 aluminum alloys under dynamic impact loading," *Mater. Sci. Eng. A*, vol. 636, pp. 379–388, 2015.
- [26] James K. Stewart, "NIJ 0108.01 - Ballistic Resistant Protective Materials," US: National Institute of Justice, Washington, 1985.
- [27] Fire A, Publication A. "NATO/PFPUN classified NATO international staff - defence investment division allied NATO reaction-to-fire tests for materials policy for the pre-selection of materials for military applications," STANAG 4602 Allied Fire Assessment Publication (AFAP), vol. 1, edition 3, July, 2010.
- [28] Arvidsson PG. NATO "Infantry Weapons Standardization". NATO Army Armaments Group; Brussels, Belgium, 2008.
- [29] M. Safety and I. Analysis, "STANAG 4241: Review of the Bullet Impact Test Background," US: Munitions Safety Information Analysis Center; San Diego, 2013.
- [30] E. Haro Albuja, J. A. Szpunar, and A. G. Odeshi, "Ballistic impact response of laminated hybrid materials made of 5086-H32 aluminum alloy, epoxy and Kevlar® fabrics impregnated with shear thickening fluid," *Compos. Part A Appl. Sci. Manuf.*, vol. 87, pp. 54–65, 2016.
- [31] E. E. Haro, A. G. Odeshi, and J. A. Szpunar, "The energy absorption behavior of hybrid composite laminates containing nano-fillers under ballistic impact," *Int. J. Impact Eng.*, vol. 96, pp. 11–22, May 2016.
- [32] S. Abrate, "Impact engineering of composite structures," *CISM Courses and Lectures*, vol. 526, Springer Wien, New York, 2011.
- [33] I. Mohagheghian, G. J. McShane, and W. J. Stronge, "Impact perforation of monolithic polyethylene plates: Projectile nose shape dependence," *Int. J. Impact Eng.*, vol. 80, pp. 162–176, 2015.
- [34] A. Ramezani Kakroodi, Y. Kazemi, and D. Rodriguez, "Mechanical, rheological, morphological and water absorption properties of maleated polyethylene/hemp composites: Effect of ground tire rubber addition," *Compos. Part B Eng.*, vol. 51, pp. 337–344, 2013.
- [35] N. A. Mohd Ayob, M. Ahmad, and N. N. Mohd Khairuddin, "Water Resistance and Tensile Strength of High Density Polyethylene (HDPE) Composites," *Adv. Mater. Res.*, vol. 1134, pp. 34–38, 2016.
- [36] M. Jacob, S. Thomas, and K. T. Varughese, "Natural rubber composites reinforced with sisal/oil palm hybrid fibers: Tensile and cure characteristics," *J. Appl. Polym. Sci.*, vol. 93, no. 5, pp. 2305–2312, 2004.
- [37] M. D. H. Beg, J. O. Akindoyo, S. Ghazali, and A. A. Mamun, "Impact Modified Oil Palm Empty Fruit Bunch Fiber / Poly (Lactic) Acid Composite," vol. 9, no. 1, pp. 165–170, 2015.
- [38] A. Boudenne, L. Ibos, Y. Candau, and S. Thomas, "Handbook of Multiphase Polymer Systems.", John Wiley and Sons Ltd., vol. 1., 2011.
- [39] H. Abdulhamid, A. Kolopp, C. Bouvet, and S. Rivallant, "Experimental and numerical study of AA5086-H111 aluminum plates subjected to impact," *International Journal of Impact Engineering*, vol. 51, pp. 1–12, 2013.